Iron-Mediated Inhibition of Mitochondrial Manganese Uptake Mediates Mitochondrial Dysfunction in a Mouse Model of Hemochromatosis

Hani A Jouihan,[1] Paul A Cobine,[1] Robert C Cooksey,[1,2] Emily A Hoagland,[1] Sihem Boudina,[1] E Dale Abel,[1] Dennis R Winge,[1] and Donald A McClain[1,2]

[1]Departments of Medicine and Biochemistry, University of Utah School of Medicine, Salt Lake City, Utah, USA; and [2]Veterans Administration Medical Center, Salt Lake City, Utah, USA

Previous phenotyping of glucose homeostasis and insulin secretion in a mouse model of hereditary hemochromatosis (*Hfe*$^{-/-}$) and iron overload suggested mitochondrial dysfunction. Mitochondria from *Hfe*$^{-/-}$ mouse liver exhibited decreased respiratory capacity and increased lipid peroxidation. Although the cytosol contained excess iron, *Hfe*$^{-/-}$ mitochondria contained normal iron but decreased copper, manganese, and zinc, associated with reduced activities of copper-dependent cytochrome c oxidase and manganese-dependent superoxide dismutase (MnSOD). The attenuation in MnSOD activity was due to substantial levels of unmetallated apoprotein. The oxidative damage in *Hfe*$^{-/-}$ mitochondria is due to diminished MnSOD activity, as manganese supplementation of *Hfe*$^{-/-}$ mice led to enhancement of MnSOD activity and suppressed lipid peroxidation. Manganese supplementation also resulted in improved insulin secretion and glucose tolerance associated with increased MnSOD activity and decreased lipid peroxidation in islets. These data suggest a novel mechanism of iron-induced cellular dysfunction, namely altered mitochondrial uptake of other metal ions.

Online address: http://www.molmed.org
doi: 10.2119/2007-00114.Jouihan

INTRODUCTION

Hereditary hemochromatosis (HH) is a common autosomal recessive disorder of iron metabolism (1,2). The majority of individuals with HH are homozygous for a single nucleotide substitution (C282Y) in the hemochromatosis gene (*HFE*) (3). Normal HFE protein expression is required for hepatic synthesis of hepcidin, a peptide that regulates iron absorption in a negative feedback loop through the downregulation of the iron channel ferroportin (4). Patients with HH are characterized by excessive intestinal absorption of dietary iron leading to systemic iron overload in multiple organs which may result in cirrhosis, diabetes, and cardiac failure (1,5–7). It is assumed, but unproven, that the progressive accumulation of iron in tissues of HH patients is directly responsible for complications via iron's established role in promoting tissue damage by free radical-mediated mechanisms (8–10).

Although diabetes is part of the classic clinical presentation of hemochromatosis, its pathogenesis is not fully understood. We have demonstrated previously that mice with targeted deletion of the hemochromatosis gene (*Hfe*$^{-/-}$) (11), like humans with HH (5), exhibit decreased insulin secretion. The mouse islets show evidence of oxidative stress, apoptotic loss of β cell mass, and desensitization of glucose-induced insulin secretion secondary to iron accumulation (11). Because of the crucial roles of mitochondria in both apoptosis and glucose-stimulated insulin secretion, we hypothesized that iron might result in mitochondrial dysfunction. Herein, we demonstrate that in the liver of *Hfe*$^{-/-}$ mice, iron accumulates mainly in the cytosol but not in mitochondria. Mitochondrial manganese, copper, and zinc, however, are decreased significantly. This is associated with reductions in mitochondrial oxygen consumption, the activities of mitochondrial manganese-dependent superoxide dismutase (MnSOD), and copper-dependent cytochrome c oxidase (CCO). This mitochondrial dysfunction is reversible with manganese supplementation, which normalizes lipid peroxidation and MnSOD activity, and leads to enhanced insulin secretory capacity and improved glucose tolerance in *Hfe*$^{-/-}$ mice.

Address correspondence and reprint requests to *D A McClain, Division of Endocrinology and Metabolism, University of Utah School of Medicine, 30 North 2030 East, Salt Lake City, UT 84132. Phone: 801-585-0954; Fax: 801-585-0956; E-mail: donald.mcclain@hsc.utah.edu.*
Submitted November 8, 2007; Accepted for publication December 28, 2007; Epub (www.molmed.org) ahead of print December 28, 2007.

MATERIALS AND METHODS

Experimental Animals

Mice with targeted deletion of the mouse hemochromatosis gene (*Hfe*$^{-/-}$) (12,13) were bred onto the 129/SvEvTac

strain for at least eight generations. Dietary iron overload was produced by supplementing the diet with 20 g/kg carbonyl iron (Harlan Teklad TD91013) for a period of 2 months. Manganese supplementation was achieved by a daily intraperitoneal (i.p.) injection of 250 µL of 30 mM $MnCl_2$ in sterile saline (0.9 %). Control mice were injected with sterile saline. Female *Hfe*$^{-/-}$ mice were used at 8 to 10 months of age and age-matched wild type 129/SvEvTac littermates (*Hfe*$^{+/+}$) were used as controls. Procedures were approved by the Institutional Animal Care and Use Committee of the University of Utah.

Isolation of Mitochondria

Fresh mouse livers were minced and homogenized at 4°C in 250 mM sucrose, 5 mM Tris/HCl and 2 mM EGTA, pH 7.4 (for respiration assays) or 250 mM sucrose, 10 mM HEPES, 0.5 mM EGTA, 0.1% BSA, pH 7.4 (for other assays). Homogenization utilized four to six strokes with a Dounce homogenizer in isolation medium (10 mL/g tissue). The homogenates were centrifuged at 1,000*g* for 3 min at 4°C. The supernatants were centrifuged (12,000*g*, 10 min) to obtain a crude mitochondria pellet. These pellets were washed in 10 mL of isolation buffer (without BSA and EGTA), recentrifuged, and resuspended in isolation buffer. Protein concentrations were determined using the Bio-Rad Bradford assay kit (Hercules, CA, USA). Isolation of pure mitochondria was performed using a discontinuous Histodenz (Sigma St. Louis, MO, USA) gradient (16% on 28%) as described previously (14). Integrity of mitochondrial preparations was verified by the presence of MnSOD and cytochrome c oxidase enzyme activity in mitochondrial, but not cytosolic, fractions. The primarily cytosolic Cu/Zn-SOD activity was not detected in mitochondrial fractions, confirming their purity.

Measurement of Mitochondrial Oxygen Consumption

Oxygen consumption in isolated liver mitochondria was measured using a fiber-optic oxygen sensor (Ocean Optics, Orlando, FL, USA) as described (15). Mitochondrial protein (1–2 mg) was suspended in 2.0 mL of 120 mM KCl, 3 mM HEPES, 5 mM KH_2PO_4, 1 mM EGTA, and 1 mg/mL free fatty acid BSA, pH 7.2. Respiration assay was performed in a thermostated (25°C), water-jacketed, sealed glass chamber with constant magnetic stirring. Oxygen consumption rates were measured for each of the following substrates: 5 mM glutamate + 2 mM malate and 5 mM succinate + 10 mM rotenone in the basal state (state 2), following the addition of 1 mM ADP (to maximally stimulate the respiration, state 3), and in the presence of 1 µg/mL oligomycin to block ATP synthesis (state 4). Respiratory control ratios (RCR) were calculated as the ratio of respiration rate in state 3 to that in state 4.

Determination of Mitochondrial Enzyme Activities

Cytochrome c oxidase (CCO) assay was performed in the presence of 32 mM exogenously reduced cytochrome c in 40 mM potassium phosphate (pH 6.7) and 0.5% Tween 20 (14). The CCO activity was calculated by recording the oxidation of reduced cytochrome c at 550 nm, expressed as nmol oxidized cytochrome c/min/mg of protein. Succinate dehydrogenase (SDH) activity was measured using 10–50 mg crude mitochondrial proteins in a total volume of 1 mL of 50 mM potassium phosphate (pH 7.6), 5 mM EDTA, 1 mM KCN, 25 mM sodium succinate, 0.12 mM cytochrome c, and 0.12 mM phenazine methosulfate (PMS), and expressed as arbitrary units (change in A_{550}/min/mg protein) (16). Aconitase activity was measured in 50 mM Tris-HCl (pH 7.5) containing 20 mM cis-aconitic acid. The rate of change of absorbance was followed for 10 min at 240 nm, with the activity expressed as mmol cis-aconitate used/min/mg of protein. Malate dehydrogenase (MDH) activity was measured by following the rate of oxidation of NADH in the presence of oxaloacetate (17). An extinction coefficient for NADH of 6.22 mM^{-1} cm^{-1} at 340 nm was used to calculate the enzyme activity (nmol/min/mg of protein). Total SOD and MnSOD activities were assessed using a Superoxide Dismutase Assay Kit according to the manufacturer's protocol (Cayman Chemical, Ann Arbor, MI, USA). One unit of SOD is defined as the amount of enzyme needed to exhibit 50% dismutation of the superoxide radical.

Immunoblotting Analysis

Equal amounts of mitochondrial protein extracts or FPLC-purified mitochondrial fractions were electrophoresed through a 12% polyacrylamide gel and electroblotted to a polyvinylidene fluoride membrane (Bio-Rad, Hercules, CA, USA). Membranes were immunostained first with rabbit anti-MnSOD polyclonal antibody (Upstate, Lake Placid, NY, USA) or with mouse anti-porin (human mitochondrial) polyclonal antibody (Molecular Probes, Eugene, OR, USA) as a control, and then with HRP-conjugated secondary antibodies. Proteins were detected using a chemiluminescence system (PerkinElmer, Boston, MA, USA). Densitometry measurements were obtained using a UMAX Astra 3450 scanner (UMAX Technologies, Fremont, CA, USA) and NIH Image 1.63 (Bethesda, MD, USA).

Inductively Coupled Plasma Optical Emission Spectroscopy (ICP-OES) Analysis

Equal amounts of mitochondria were acid-digested for 1 h in sealed tubes at 95°C in 150 mL of metal free 40% nitric acid (Optima, PerkinElmer, Boston, MA, USA) as described (14). As controls, blanks of nitric acid were digested in parallel. Samples were centrifuged (22,000 g, 15 min, 4°C) and supernatants were diluted to 600 µL using double-distilled water. Metal concentrations by ICP-OES (Optima 3100XL, PerkinElmer) were determined from a standard curve using metal standards (Optima, PerkinElmer).

Chromatographic Fractionation of Mitochondrial Proteins

Equal amounts of crude mitochondria from *Hfe*$^{-/-}$ and control mice were sonicated (3×30 sec pulses, 50% output, Ultrasonic W-380, Misonix, Farmingdale, NY, USA). After centrifugation (22,000 g, 15 min), soluble fractions were diluted into Buffer A (50 mM ammonium-acetate, pH 8.5), filtered (0.45 mM), and loaded onto a HR10/10 MonoQ column (Amersham Biosciences, Piscataway, NJ, USA) equilibrated in 10 column volumes (CV) of Buffer A. After washing with 5 CV of Buffer A, a 25 CV gradient (0–100%) of Buffer B (1 M ammonium-acetate, pH 8.5) was initiated. Fractions containing MnSOD protein were fractionated further by size-exclusion (HR 10/30 Superdex-200, Amersham Biosciences) in 20 mM Tris (pH 8.5) and 100 mM NaCl. All fractions were analyzed by ICP-OES and 150 mL aliquots were concentrated by speed drying for determination of MnSOD protein content by immunoblotting.

Thiobarbituric Acid Reactive Substances (TBARS) Assessment

TBARS levels were measured to assess lipid peroxidation (18–20) according to the manufacturer's protocol (OXItek TBARS Assay Kit, Zeptometrix, Buffalo, NY, USA).

Quantitation of Transcript Levels by RT-PCR

After a 17 h fast, mice were killed and livers isolated and processed as described (11). First strand cDNA synthesis was performed on RNA samples (1.5 mg/ea) using SSRTII reverse transcriptase (Invitrogen, Carlsbad, CA, USA) according to manufacturer's protocol and utilizing 125 pM T14VN oligo-dT first-strand primers (21). Real-time PCR for MnSOD and two normalizer transcripts (Cyclophilin-A and RPL13a) was performed as described (22). Primers for mouse MnSOD were, 5′ -GCCAC CGAGGAGAAGTACCA-3′ and 5′ -GCTTGATAGCCTCCAGCAACTC-3′, amplifying a 178-bp product. Eight point log-linear standard curves from compilation cDNA were generated within each PCR run, and normalization to the average of the two normalizer transcripts was applied as described (11).

Intraperitoneal Glucose Tolerance Testing (IPGTT) and Insulin Determination in vivo

After a 6 h fast, glucose (1 g/kg body weight) was administered intraperitoneally to nonsedated animals. Tail vein blood (3 µL) was sampled at 0–120 min for glucose determination (Glucometer Elite, Bayer Corp., Tarrytown, NY, USA). Blood (50 µL) also was collected at 0 and 30 min for insulin determination (Sensitive Rat Insulin Kit, Linco Research, St. Charles, MO, USA).

Preparation of Islets

Islets were isolated after collagenase digestion as described (23). Islets were separated from acinar tissue on a discontinuous Ficoll gradient.

Statistical Procedures

Descriptive statistics are represented as average ± standard error. The unpaired student *t*-test (two tail) was used to compare differences between experimental and control groups.

RESULTS

Mitochondrial Function in Liver of *Hfe*$^{-/-}$ Mice

Because the insulin secretion abnormalities in iron-overloaded *Hfe*$^{-/-}$ mice are suggestive of mitochondrial dysfunction (11), we assessed mitochondrial function in *Hfe*$^{-/-}$ mice and wild type controls. We used mitochondria from liver because that tissue is iron-overloaded in the *Hfe*$^{-/-}$ mice to a similar degree as islets (11) and the tissue provides sufficient amounts of mitochondria for functional assays. Total mitochondrial yield in preparations from *Hfe*$^{-/-}$ and wild type mice were similar: 11.7 ± 1.5 mg of mitochondrial protein/g wet liver of wild type compared with 13.0 ± 1.4 mg of mitochondrial protein/g wet liver of *Hfe*$^{-/-}$ mice ($P = 0.5$). Mitochondrial function was analyzed by measuring the rates of oxygen consumption utilizing two substrates (glutamate/malate and succinate) which serve as functional markers for electron transport complexes I and II, respectively. Compared with wild type mice, mitochondria from liver of *Hfe*$^{-/-}$ mice exhibited reduced mitochondrial respiration. Under glutamate/malate-supported respiration, states 2, 3, and 4 mitochondrial respiration were reduced by 51% ($P < 0.01$), 27% ($P < 0.05$), and 37% ($P < 0.01$), respectively (Figure 1A). Similar reductions in *Hfe*$^{-/-}$ mitochondrial respiration were found when succinate was used as substrate: States 2, 3, and 4 respiration were reduced by 33% ($P < 0.01$), 19% ($P < 0.05$), and 31% ($P < 0.01$), respectively (Figure 1B). Because oxygen consumption rates during state 3 and state 4 were reduced proportionally, the respiratory control ration (RCR) did not differ in *Hfe*$^{-/-}$ mice compared with controls (Figure 1A–B). The reduction in mitochondrial respiration was not associated with decreased protein levels of subunits of electron transport chain complexes (complex I: 30 kDa iron-sulfur protein 3, and 39 kDa α-subcomplex 9; complex II: 30 kDa iron–sulfur protein; and complex IV: 57 kDa COX1, data not shown).

Elevated Levels of Lipid Peroxidation in Liver Mitochondria from *Hfe*$^{-/-}$ Mice

Reduced mitochondrial respiration can result in enhanced oxidative damage (24,25). To determine whether liver mitochondria from the *Hfe*$^{-/-}$ mice exhibited increased oxidative damage, we determined the levels of thiobarbituric acid reactive substances (TBARS), a marker of non-specific lipid peroxidation (18–20). Liver mitochondria from *Hfe*$^{-/-}$ mice had a 61% increase in TBARS compared with controls (Figure 1C; 0.132 ± 0.012 vs. 0.082 ± 0.01 nM malondialdehyde (MDA)/mg protein; $P < 0.05$).

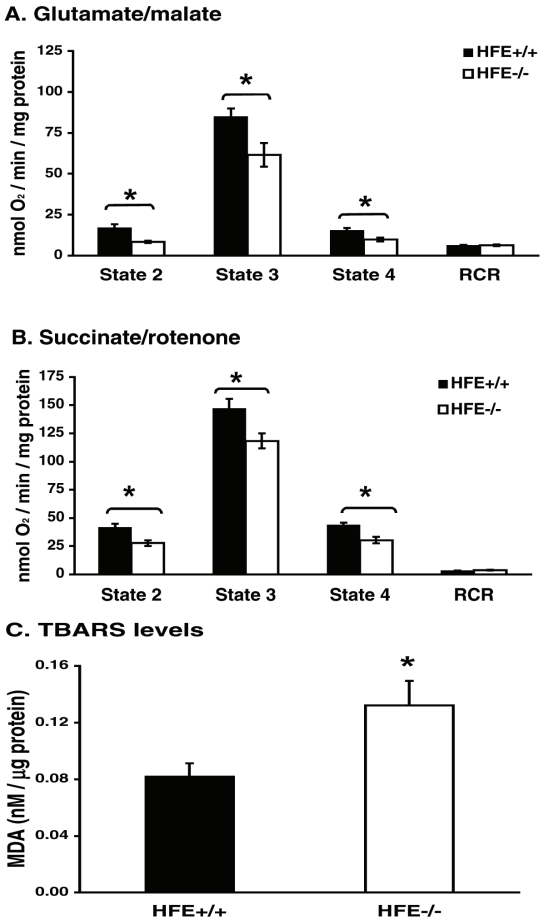

Figure 1. Lower respiratory activity and increased lipid peroxidation in isolated liver mitochondria from *Hfe*$^{-/-}$ mice. Respiration was measured in liver mitochondria from *Hfe*$^{+/+}$ and *Hfe*$^{-/-}$ mice using either glutamate/malate (A) or succinate/rotenone (B) as substrate. Rates of oxygen consumption during states 2, 3, and 4 were expressed as nmol O_2/min/mg protein and values reported are means ± SEM of 8–10 experiments. RCR, respiratory control ratio. *$P < 0.05$ compared with wild type, $n = 8$–10/group. C. Lipid peroxidation in liver mitochondria from *Hfe*$^{-/-}$ mice compared with wild type controls. Values are represented as the mean ± SEM and are expressed as nM equivalent of malondialdehyde (MDA) normalized to mitochondrial protein content per sample (*$P < 0.05$ compared with wild type, $n = 5$ for controls and $n = 6$ for *Hfe*$^{-/-}$ mice).

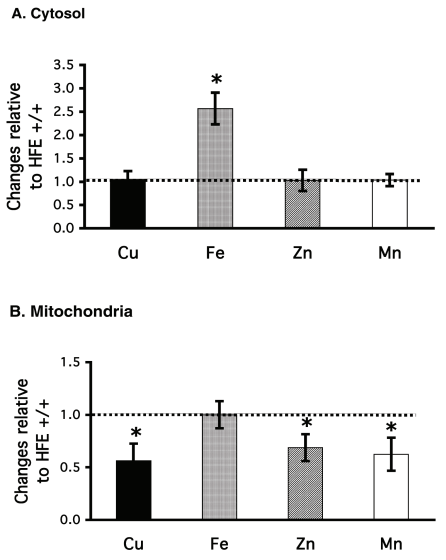

Figure 2. Metal content in cytosolic and mitochondrial liver preparations. Cytosolic and gradient-purified mitochondrial preparations were isolated from livers of *Hfe*$^{-/-}$ and *Hfe*$^{+/+}$ control mice. Values from *Hfe*$^{-/-}$ mice were normalized to wild type values and data represent the percent change in *Hfe*$^{-/-}$ mice compared with control mice (*$P < 0.01$, $n = 9$–12 independent determinations per group, with each assay using mitochondria pooled from two to three livers). A. Cytosolic content of copper, iron, zinc, and manganese from *Hfe*$^{-/-}$ mice relative to wild type controls. B. Mitochondrial metal content from *Hfe*$^{-/-}$ mice relative to wild type controls.

Altered Content of Transition Metals in Cytosolic and Mitochondrial Fractions from Livers of *Hfe*$^{-/-}$ Mice

We have reported previously that iron levels in total liver homogenates from *Hfe*$^{-/-}$ mice were elevated compared with wild type controls (11). We therefore sought to determine if iron also might be accumulating in the mitochondria to account for the respiratory defect in *Hfe*$^{-/-}$ mitochondria. Cytosolic fractions from *Hfe*$^{-/-}$ mice had significantly increased iron levels compared with wild type controls (Figure 2A; 157%, $P < 0.001$). However, normal levels of iron were observed in gradient-purified mitochondria of the *Hfe*$^{-/-}$ mice (Figure 2B). In contrast, mitochondria from *Hfe*$^{-/-}$ livers exhibited significant decreases in copper (44%), manganese (38%), and zinc (30%) compared with wild type animals (Figure 2B, $P < 0.01$). Cytosolic content of copper (+4%), manganese (+3%), and zinc (+3%) in *Hfe*$^{-/-}$ liver were not significantly different from wild type mice (Figure 2A).

Reduced Mitochondrial Cytochrome C Oxidase and Manganese Superoxide Dismutase Activities in *Hfe*$^{-/-}$ Mice

We next sought to determine if the reduction of mitochondrial manganese and copper were functionally significant by measuring the activities of copper-dependent cytochrome c oxidase (CCO) and the manganese-containing superoxide dismutase (MnSOD or SOD2) in liver mitochondria from wild type and *Hfe*$^{-/-}$ mice. *Hfe*$^{-/-}$ mice had a 21% decrease in mitochondrial CCO activity compared with controls (Figure 3A, 4.06 ± 0.17 vs. 5.12 ± 0.37 nmol/min/mg protein, $P < 0.05$) and a 25% reduction in mitochon-

drial MnSOD (Figure 3B, 3.34 ± 0.35 vs. 4.44 ± 0.33 units SOD2/mg protein, $P < 0.05$). The reduction in MnSOD activity was not associated with decreased levels of either mitochondrial MnSOD protein (12.9 ± 1.19 densitometry arbitrary units in wild types-verses-13.5 ± 2.4 in $Hfe^{-/-}$ mice, $n = 6$/group, $P = 0.8$) or mRNA (relative levels of 1.00 ± 0.10 in wild type, $n = 7$ compared with 1.01 ± 0.07 in $Hfe^{-/-}$, $n = 8$, $P = 0.9$). CCO and MnSOD activities were not detected in cytosolic fractions (data not shown), confirming that the purification procedure generated intact mitochondria without leakage of CCO or MnSOD into cytosol. Activity of malate dehydrogenase (MDH), a non-metal containing enzyme of the mitochondrial tricarboxylic acid cycle, was not different between $Hfe^{-/-}$ mice and wild type controls (Figure 3C, 18.6 ± 2.8 vs. 18.8 ± 2.8 nmol/min/mg protein, $P = 0.7$).

Normal mitochondrial aconitase and succinate dehydrogenase activities in $Hfe^{-/-}$ mice. Aconitase and succinate dehydrogenase (SDH) are iron-sulfur-containing enzymes that are susceptible to inactivation by superoxide radicals (26). Mitochondrial aconitase activities in $Hfe^{-/-}$ mice were not reduced, however, compared with controls (0.62 ± 0.14 mmol/min/mg protein in wild type-verses-0.65 ± 0.15 mmol/min/mg protein in $Hfe^{-/-}$ mice, $n = 11$, $P = 0.9$), nor were SDH activities (0.079 ± 0.027 unit SDH/min/mg protein in wild type vs. 0.078 ± 0.015 unit SDH/min/mg protein in $Hfe^{-/-}$ mice, $n = 8$–10, $P = 0.85$).

Wild type mice with dietary iron overload also display abnormal mitochondrial metal distribution and function. The altered mitochondrial levels of copper, manganese, and zinc may arise from the cytosolic iron accumulation in $Hfe^{-/-}$ mice or from a function of the HFE protein. To address this question, we subjected wild type $Hfe^{+/+}$ mice to either normal chow (NC) or a diet supplemented with carbonyl iron to induce tissue iron overload. Cytosolic fractions from wild type mice fed excess dietary iron displayed high iron levels compared with NC-fed wild type controls (Figure 4A; +770%, $P < 0.01$), yet cytosolic levels of copper (+16%), manganese (–16%), and zinc (+9%) in livers of iron-fed mice were not significantly different from NC-fed animals (Figure 4A). The increase in cytosolic iron was significantly greater than that seen in the $Hfe^{-/-}$ mice (Figure 2A), and was also associated with elevated mitochondrial iron content in iron-fed wild type mice (Figure 4B; +102%, $P < 0.03$). Mitochondria from wild type mice fed excess dietary iron also displayed significant decreases in copper (–18%,

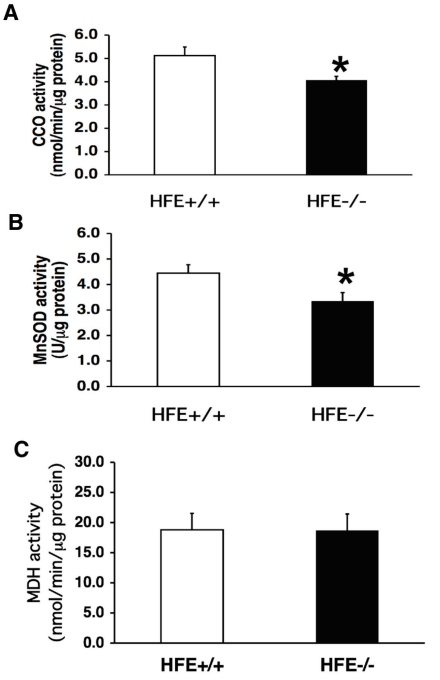

Figure 3. Mitochondrial enzyme activities. Crude mitochondria were isolated from livers of $Hfe^{-/-}$ mice (open bars) and $Hfe^{+/+}$ controls (black bars). Values are represented as the mean ± SEM. A. Activity of CCO was reduced significantly in $Hfe^{-/-}$ mice (4.06 ± 0.17 vs. 5.12 ± 0.37 nmol oxidized cytochrome c/min/mg protein, 6–7 mice/group, $^*P < 0.05$). B. Activity of MnSOD was reduced in $Hfe^{-/-}$ mice (3.34 ± 0.35 vs. 4.44 ± 0.33 unit SOD/mg protein, 7–9 mice/group, $^*P < 0.05$). C. MDH activity showed no difference between $Hfe^{-/-}$ mice and wild type controls (18.6 ± 2.8 vs. 18.8 ± 2.8 nmol NADH used/min/mg protein, 6–7 mice/group, $P = 0.7$).

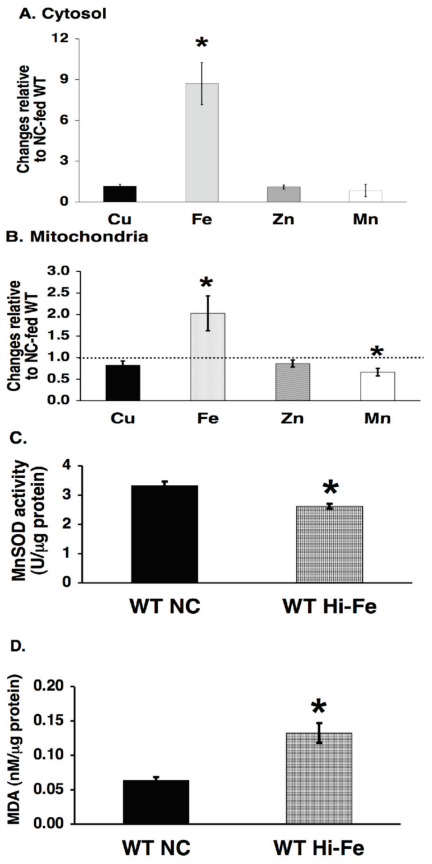

Figure 4. Altered metal distribution, MnSOD activity, and lipid peroxidation in liver preparations from wild type mice fed excess dietary iron. Cytosolic (A) and gradient-purified mitochondrial (B) preparations were isolated from livers of age-matched (8–10 month old) male wild type mice fed either normal chow (WT-NC) or excess dietary iron (WT Hi-Fe). Contents of copper, iron, zinc, and manganese from iron-fed mice were normalized to WT-NC values and data represent the percent change in iron-fed mice compared with NC-fed wild type mice ($^*P < 0.05$, $n = 4$–9 independent determinations per group, with each assay using mitochondria pooled from two to three livers). C. Activity of mitochondrial MnSOD was reduced in iron-fed $Hfe^{+/+}$ mice (2.62 ± 0.08 for iron-fed mice vs. 3.32 ± 0.15 unit SOD/mg protein for controls, 4 mice/group; $^*P < 0.01$). Values are represented as the mean ± SEM. D. TBARS in iron-fed $Hfe^{+/+}$ mice were elevated compared with NC-fed controls (0.13 ± 0.01 compared with 0.06 ± 0.005, 4 mice/group; $^*P < 0.01$).

$P < 0.05$) and manganese (–34%, $P < 0.01$) (Figure 4B). Zinc levels were 14% lower than NC-fed control animals, but that difference was not statistically significant ($P = 0.12$; Figure 4B). Mitochondria from iron-fed wild-type mice had a 21% decrease in mitochondrial MnSOD activity (Figure 4C; 2.62 ± 0.08 compared with 3.32 ± 0.15 unit SOD2/mg protein, $P < 0.01$) without a change in MnSOD protein (not shown). Liver mitochondria from iron-fed wild type mice also had a 109% increase in lipid peroxidation (TBARS) compared with NC-fed controls (Figure 4D; 0.132 ± 0.014 vs. 0.063 ± 0.014 nM MDA/mg protein; $P < 0.005$).

Decrease in SOD-Bound Manganese in Mitochondria from Livers of *Hfe*$^{-/-}$ Mice

To assess whether the decrease in mitochondrial manganese was directly responsible for the observed reduction in MnSOD activity in *Hfe*$^{-/-}$ mice, we purified MnSOD and determined the degree of metallation of this protein. Soluble components of liver mitochondria from wild type and *Hfe*$^{-/-}$ mice were subjected to Mono Q anion exchange FPLC followed by size exclusion chromatography (Figure 5A). Immunoblotting was utilized to detect mitochondrial MnSOD protein and metal levels were assessed by ICP-OES. A manganese-containing peak coeluted with the bulk of SOD protein in wild type and *Hfe*$^{-/-}$ mitochondrial preparations (Figure 5A–B). In *Hfe*$^{-/-}$ mitochondrial preparations, the manganese content normalized to the eluted SOD protein was reduced by 54% compared with wild type controls (Figure 5C, $P = 0.02$). Although this degree of decrease in Mn associated with MnSOD in *Hfe*$^{-/-}$ mice is larger than the observed decrease in intramitochondrial Mn (38%, Figure 2) and the decrease in MnSOD activity (25%, Figure 3), the relative decreases in these three measures are not significantly different from one another. Only trace amounts of iron coeluted with the bulk of SOD protein, with no difference between wild type and *Hfe*$^{-/-}$ fractions. A second manganese-containing

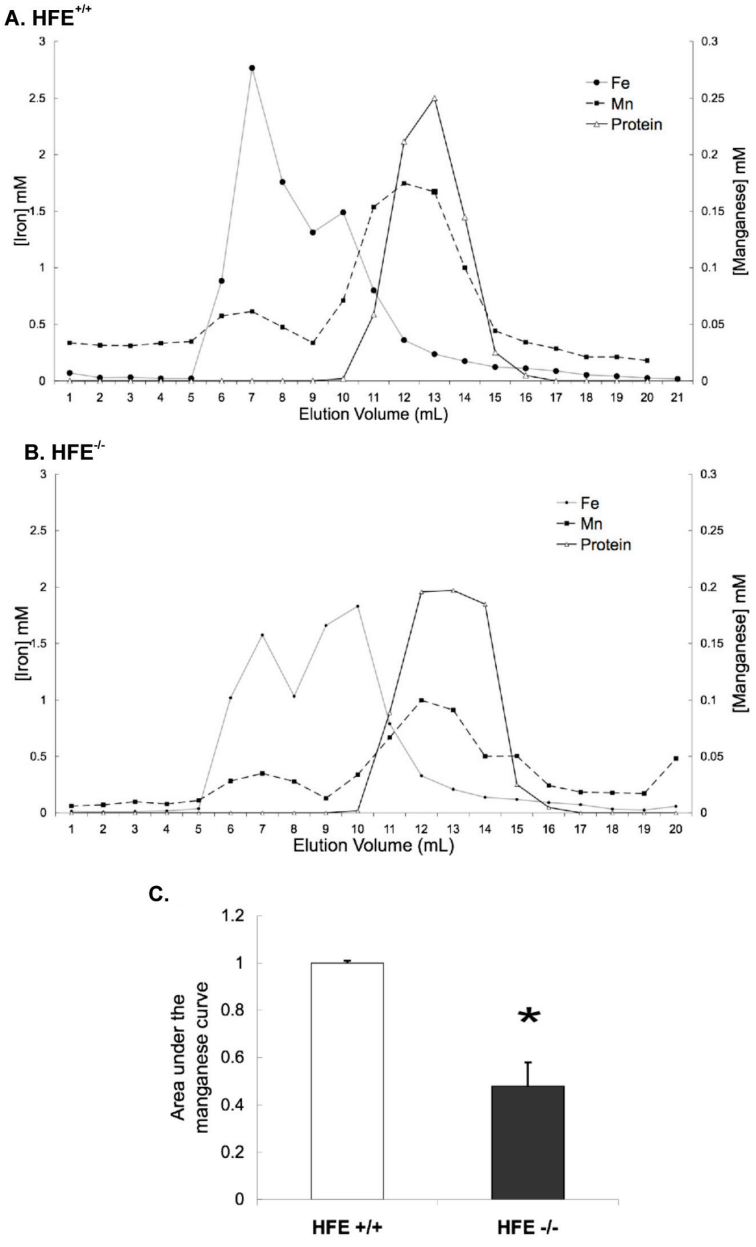

Figure 5. Reduced amounts of manganese associated with SOD protein in mitochondria from livers of *Hfe*$^{-/-}$ mice. SOD protein was purified from equal amounts of crude mitochondrial protein extracts of *Hfe*$^{-/-}$ and control mice by anionic exchange followed by size exclusion FPLC fractionation. Measurement of manganese and iron content in 1 mL fractions following size exclusion was performed by ICP-OES. Immunoblotting with MnSOD antibody was utilized to determine SOD protein content and final values were measured as arbitrary densitometric units (range 0.0 to 0.3). A. Manganese (black squares and dashed line), iron (black circles and dotted line), and MnSOD protein (open triangles and solid line) in mitochondrial fractions from wild type mice (average of three independent determinations). B. Manganese, iron, and MnSOD protein levels in mitochondrial fractions from *Hfe*$^{-/-}$ mice. C. Incremental areas under manganese curves were calculated and normalized to SOD protein (measured as arbitrary densitometric units). SOD-bound manganese was decreased by 54% in mitochondria from liver of *Hfe*$^{-/-}$ mice compared with control mice ($P = 0.02$, $n = 3$/group).

peak (fractions 5–8, Figure 5A–B) was seen inconsistently in both mice groups, but this peak was not associated with SOD protein and thus represents either an artifact or a manganese-containing component of unknown identity.

Manganese supplementation reverses mitochondrial manganese deficiency and restores MnSOD activity in *Hfe*$^{-/-}$ mice. Because the observed reduction in mitochondrial manganese content in *Hfe*$^{-/-}$ mice was associated with under-metallation and decreased activity of MnSOD, we hypothesized that supplementing manganese might reverse these defects. Manganese supplementation was achieved by daily intraperitoneal injections of $MnCl_2$ for 1 week. We determined the distribution of manganese and iron in cytosolic and gradient-purified mitochondrial fractions prepared from livers of mock-treated and the manganese-supplemented *Hfe*$^{-/-}$ mice. Iron content in both cytosol and mitochondria were similar in manganese-supplemented *Hfe*$^{-/-}$ mice compared with mock-treated *Hfe*$^{-/-}$ controls (Figure 6A). Manganese treatment, however, resulted in 14- and 20-fold increases in cytosolic and mitochondrial manganese, respectively (Figure 6B). This increase in mitochondrial manganese resulted in a 192% increase in mitochondrial MnSOD activity (Figure 6C, 9.76 ± 0.45 compared with 3.34 ± 0.35 unit SOD/mg protein, $P < 0.001$) in manganese supplemented *Hfe*$^{-/-}$ mice without affecting mitochondrial MnSOD protein levels (data not shown). The enhancement in MnSOD activity had a protective effect. Manganese supplemented *Hfe*$^{-/-}$ mice had a 54% decrease in lipid peroxidation as assessed by mitochondrial TBARS levels, compared with mock-treated *Hfe*$^{-/-}$ controls (Figure 6D; 0.06 ± 0.007 compared with 0.13 ± 0.017 nM MDA/mg protein; $P < 0.01$).

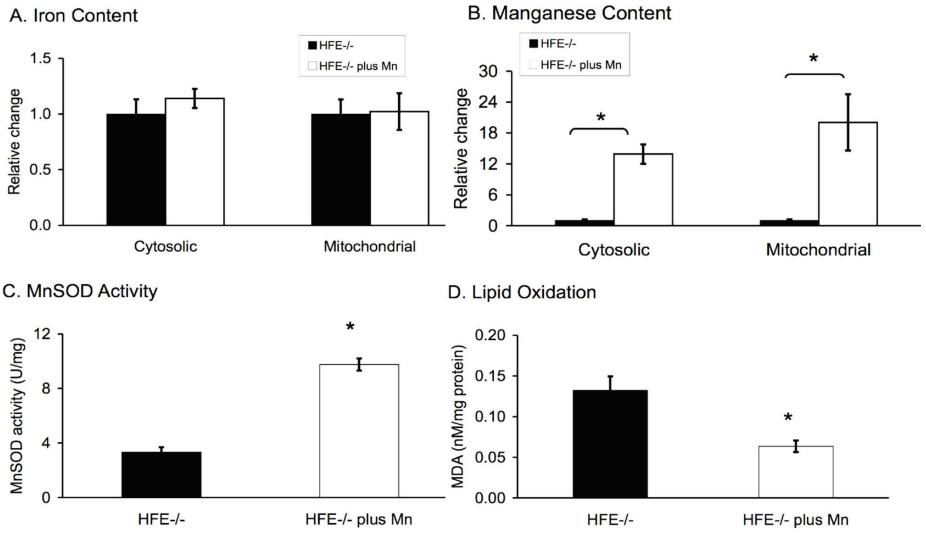

Figure 6. Manganese supplementation reverses mitochondrial phenotype of the *Hfe*$^{-/-}$ mice. Liver cytosolic and gradient-purified mitochondrial preparations were isolated from *Hfe*$^{-/-}$ mice that either were mock controls or manganese-treated (plus Mn). Figures show contents of cytosolic and mitochondrial iron and manganese from *Hfe*$^{-/-}$ mice (plus Mn) (hatched bars) presented as the percent change in (plus Mn) *Hfe*$^{-/-}$ mice compared with controls (open bars). A. Iron content in cytosolic and mitochondrial preparations from *Hfe*$^{-/-}$ mice (plus Mn) displayed no changes compared with mock-treated *Hfe*$^{-/-}$ mice. Actual iron values were: cytosol, 24.7 ± 1.9 nmol iron/mg protein for (plus Mn) mice compared with 21.7 ± 2.9 for controls; mitochondria, 13.6 ± 2.2 nmol iron/mg protein for (plus Mn) mice compared with 13.4 ± 1.7 for controls; P = NS; n = 4–6 determinations/group). Values are represented as the mean ± SEM. B. Manganese supplementation caused significant manganese accumulation in cytosolic and mitochondrial preparations in (plus Mn) *Hfe*$^{-/-}$ mice compared with controls. Actual manganese values were: cytosol, 0.4 ± 0.06 nmol Mn/mg protein for (plus Mn) mice compared with 0.03 ± 0.007 for controls, in mitochondria, 1.62 ± 0.4 nmol Mn/mg protein for (plus Mn) mice compared with 0.08 ± 0.02 for controls; *$P < 0.001$; n = 4–6 determinations/group). C. Manganese supplementation increases activity of mitochondrial MnSOD in *Hfe*$^{-/-}$ mice compared with controls (9.76 ± 0.45 vs. 3.34 ± 0.35 unit SOD/mg protein, 7–9 mice/group; *$P < 0.001$). D. Manganese (plus Mn) supplementation reduced TBARS levels in *Hfe*$^{-/-}$ mice compared with untreated controls (0.06 ± 0.01 compared with 0.13 ± 0.02, 6–8 mice/group; *$P < 0.01$).

Manganese supplementation improves glucose-induced insulin secretion and glucose tolerance in *Hfe*$^{-/-}$ mice. Our original hypothesis was that the decrease in insulin secretion in *Hfe*$^{-/-}$ mice was due to mitochondrial dysfunction (11). If similar effects to those described for liver (Figure 6) also occurred in islets, we predicted that manganese supplementation should improve insulin secretion and glucose tolerance in *Hfe*$^{-/-}$ mice. Insulin levels 30 min following intraperitoneal glucose challenge were significantly higher in the manganese-treated *Hfe*$^{-/-}$ mice than in the mock-treated *Hfe*$^{-/-}$ controls (Figure 7A, 52% increase, 0.79 ± 0.05 compared with 0.52 ± 0.03 ng/mL insulin, $P < 0.01$). Manganese-treated *Hfe*$^{-/-}$ mice also showed a trend toward increased fasting serum insulin levels (Figure 7A, 25% increase, 0.40 ± 0.05 compared with 0.32 ± 0.02 ng/mL insulin, $P = 0.18$). In the face of increased insulin, fasting glucose levels and levels 60 and 120 min after glucose challenge were significantly lower in manganese-supplemented *Hfe*$^{-/-}$ mice compared with mock-treated *Hfe*$^{-/-}$ mice (Figure 7B, 82 ± 3.5 compared with 98 ± 2.4 mg/dl fasting glucose levels, 105 ± 14.1 compared with 147 ± 11.1 mg/dl glucose at 60 min, and 86 ± 8.3 compared with 120 ± 5.4 mg/dl glucose at 120 min, $P < 0.01$). We also confirmed that manganese supplementation of the *Hfe*$^{-/-}$ mice led to increased MnSOD activity in islets (Figure 7C, 56% higher than *Hfe*$^{-/-}$ controls, $P < 0.05$) and

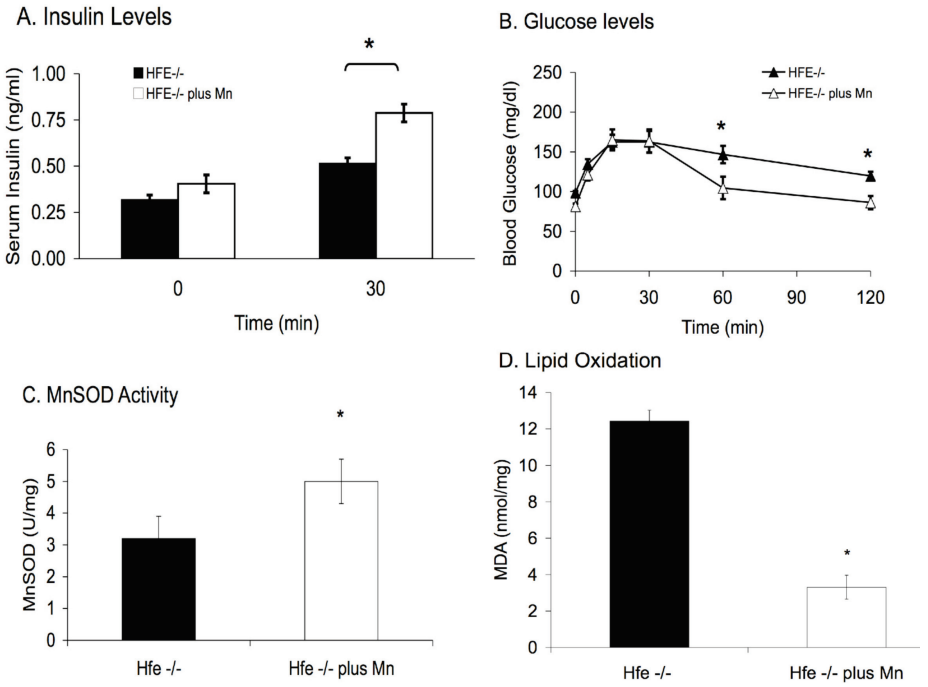

Figure 7. Manganese supplementation improves insulin secretion, glucose tolerance, islet MnSOD activity, and islet oxidant stress in *Hfe*$^{-/-}$ mice. Glucose (1 mg/g body weight) was administered intraperitoneally to age-matched (8–10 month old) male *Hfe*$^{-/-}$ mice that either were treated with manganese (plus Mn) or mock-treated (n = 5–6 mice/group). A. Serum insulin levels were determined before and 30 min after glucose injection (*$P < 0.01$ for (plus Mn) *Hfe*$^{-/-}$ compared with *Hfe*$^{-/-}$ controls). B. Glucose levels were determined at the indicated times (*$P < 0.01$ for (plus Mn) *Hfe*$^{-/-}$ compared with *Hfe*$^{-/-}$ controls). C. Manganese supplementation increases activity of MnSOD in islets from *Hfe*$^{-/-}$ mice compared with controls (4 mice/group; *$P < 0.05$). D. Manganese supplementation (plus Mn) reduced TBARS levels in islets from *Hfe*$^{-/-}$ mice compared with untreated controls (4 mice/group; *$P < 0.001$).

this was associated with a significant decrease in lipid oxidation as assessed by the TBARS assay (Figure 7D, 73% lower than controls, $P < 0.001$).

DISCUSSION

Mitochondria are key organelles for cellular function and survival (27–29), and mitochondrial dysfunction has been implicated in a number of diseases including neurodegenerative diseases (30), cardiomyopathy (31), and diabetes (27,32–34). Free radicals, such as reactive oxygen and nitrogen species, are normally generated during energy production in mitochondria. Excess levels of these radicals can negatively affect mitochondrial function through oxidative damage of mitochondrial macromolecules (35,36). Because non-protein-bound iron can generate free radicals through Fenton chemistry, we studied the effect of iron overload associated with hemochromatosis on oxidative damage and mitochondrial function. This study demonstrates that in a mouse model of hemochromatosis (*Hfe*$^{-/-}$), iron accumulation in the liver is confined to the cytosol where it is associated with decreased mitochondrial accumulation of other metals—including manganese, copper, and zinc. Mitochondria from *Hfe*$^{-/-}$ mice are dysfunctional and manifest increased oxidant damage, but correcting the mitochondrial manganese deficit largely reverses this damage.

The *Hfe*$^{-/-}$ mouse, like humans with hereditary hemochromatosis, exhibit β cell apoptosis and decreased glucose-stimulated insulin secretion (5,11). While it was not feasible to assess metal levels directly in mitochondria from pancreatic β cells, we have observed previously that the degree of increased iron in β cells is comparable to that observed in liver cytosol (11). In the current study, we show that the insulin secretory defect observed in the *Hfe*$^{-/-}$ mice is reversed by manganese supplementation, resulting in improved insulin secretion and, consequently, enhanced glucose tolerance. This is associated, as in liver, with increased MnSOD activity and decreased lipid peroxidation in islets from manganese-supplemented *Hfe*$^{-/-}$ mice. These results are consistent with the likelihood that β cell mitochondria exhibit the same changes in MnSOD levels observed in liver mitochondria. Furthermore, these data suggest that mitochondrial manganese availability is a limiting factor in protection against oxidative stress in this model. These observations correlate strongly with a proposed causative role of oxidative stress in several diabetes models (37).

The mitochondrial dysfunction in *Hfe*$^{-/-}$ mice, evidenced by decreased oxygen consumption, is consistent with oxidative damage and lipid peroxidation. Studies on cardiac reperfusion injury, for example, have demonstrated that treatment of cardiac mitochondria with 4-hydroxy-2-nonenal (HNE) results in decreased NADH-linked (complex-I) respiration, and other studies have implicated products of lipid peroxidation in altering cellular membrane permeability (38,39). Our data show that the iron accumulation in *Hfe*$^{-/-}$ mice occurs in the cytoplasm, but not mitochondria, suggesting that mitochondrial iron accumulation resulting in generation of reactive oxygen species by Fenton chemistry is not the major source of oxidative stress within the mitochondria. The finding that *Hfe*$^{-/-}$ mice are able to regulate iron transport into, and/or export from, mitochondria and maintain a normal pool of mitochondrial iron—despite the presence of a two-fold increase in cytosolic iron

content, has not been described previously and its mechanism is not known.

The altered mitochondrial metal profile in the *Hfe*$^{-/-}$ mice is solely a result of elevated cytosolic iron, as demonstrated by similar mitochondrial deficits of manganese, copper, and zinc in wild type mice fed excess iron. Thus the Hfe protein itself does not seem to be responsible. It is important to note that the iron-fed wild type, unlike *Hfe*$^{-/-}$ mice, accumulated excess iron in mitochondria. This is likely due to an approximately three-fold greater degree of accumulation of iron in cytosol of the iron-fed mice compared with the *Hfe*$^{-/-}$ mice. Thus the ability of the mitochondria to maintain normal iron content, seen in the *Hfe*$^{-/-}$ mice, is most likely limited to situations of modest cytosolic accumulation. Further studies of iron uptake with graded iron challenge of wild type and *Hfe*$^{-/-}$ mice will be required to answer this question. It also is noteworthy that in the wild type mice fed excess dietary iron, the degrees of diminution of mitochondrial Mn, Cu, and Zn appear to be less than in the *Hfe*$^{-/-}$ mice that exhibit a lower degree of cytosolic iron accumulation. Among possible explanations for this result are upregulation of mitochondrial metal transporters in situations of large changes in metal availability, or a heretofore undescribed function for the Hfe protein in regulation of mitochondrial metal accumulation. Answers to these questions await identification of the relevant transport proteins and an understanding of their regulation.

MnSOD plays a critical role in protecting the mitochondria from free radicals normally generated during respiration by converting superoxide anions into hydrogen peroxide, which is detoxified into water by mitochondrial glutathione peroxidase (40). Mice homozygous for deletion of MnSOD (*SOD2*$^{-/-}$) die shortly after birth due to dilated cardiomyopathy and lipid accumulation in liver and muscles (41). The heterozygous knockout mice (*SOD2*$^{+/-}$) are viable and grossly normal despite a 50% reduction of MnSOD activity in all tissues, and exhibit alterations in mitochondrial function (42–44). Our data demonstrate a 21% reduction in MnSOD activity in *Hfe*$^{-/-}$ mice, and increased mitochondrial lipid peroxidation. The decrease in MnSOD activity in the *Hfe*$^{-/-}$ mice is less than that observed in *SOD2*$^{+/-}$ mice, perhaps accounting for the normal activities of aconitase and SDH observed in *Hfe*$^{-/-}$ mice. Thus, the remaining MnSOD activity in *Hfe*$^{-/-}$ mice could be sufficient to provide some protection against oxidative damage, at least in the unstressed state. It should be noted that the phenotype of the *SOD2*$^{+/-}$ mice, in terms of glucose tolerance and insulin secretion, has not been reported. In the case of the *Hfe*$^{-/-}$ mice, however, we have determined that the decreased insulin secretion is balanced by enhanced sensitivity to insulin, resulting in overall glucose tolerance that is modestly supranormal (45). Thus, the *SOD2*$^{+/-}$ mice also might have a subtle overall metabolic phenotype that would be defined only with careful and separate dissection of glucose handling and insulin secretion.

Metallation of MnSOD occurs in the mitochondria upon translocation of manganese and the non-metal containing SOD protein from the cytosol, where the protein is activated immediately after import (40,46,47). In *Saccharomyces cerevisiae*, conditions of mitochondrial iron overload, or manganese deficiency, result in the mismetallation with iron of the MnSOD homologue, SOD2 (48). Inappropriate iron binding to MnSOD inactivates the protein because of altered redox potential (48–53). In this mouse model, however, there was no demonstrable misincorporation of iron into SOD2, even in iron-fed wild type mice that accumulate mitochondrial iron (data not shown). This suggests that the oxidative stress-related defect is due to availability of manganese rather than aberrant iron binding. We, therefore, wanted to determine the extent to which supplementing *Hfe*$^{-/-}$ mice with excess manganese might reverse this defect. Supplementing *Hfe*$^{-/-}$ mice with manganese not only leads to increased mitochondrial manganese content, but also to increased MnSOD activity and decreased oxidative damage as assessed by lipid peroxidation. This enhanced activity resulted in improved glucose homeostasis parameters. In fact, we noted that with manganese supplementation, the activity of SOD increased by greater than the 21% deficit that is observed in the *Hfe*$^{-/-}$ mice on normal chow. This result implies that SOD activity was limited by manganese availability, and not by protein levels in the liver. In support of this observation, MnSOD in wild type mice on normal chow can be enhanced by additional manganese supplementation, even in the absence of iron overload, although the fold increase is lesser in wild type mice than what is observed for the *Hfe*$^{-/-}$ mice (data not shown). Enhancement of activity with supplementation implies that a pool of apo-SOD2 is present in murine mitochondria. Previous observations in yeast suggest that this pool of apo-SOD2 cannot be activated, as manganese binding can occur only as the SOD2 is inserted into the matrix before folding (47). The murine and yeast mitochondria differ, however, in that the pool of apo-SOD2 appears to be mismetallated with iron in yeast even under wild type conditions (48). The effects of supplementing wild type mice with manganese on glucose tolerance and insulin secretion are in progress, and our preliminary data suggest a positive effect of short-term manganese supplementation on insulin secretion in wild type animals, consistent with enhanced MnSOD activity.

Our observations point out the previously unrecognized potential of manganese as a limiting factor in antioxidant defenses. Because of insufficient information on manganese requirements, the Food and Nutrition Board of the Institute of Medicine has not set a Recommended Dietary Allowance (RDA), instead setting an "adequate intake level" of 2 mg/day. Thus, optimal manganese intake levels are unknown, although excessive ingestion, as occurs in miners, can lead to neurodegenerative diseases (54). Variable levels of manganese and resulting variation

in or suboptimal levels of MnSOD also may be an issue in experimental studies. Most culture media, for example, contain no manganese so that the metal is available only from serum, which contains approximately 10 nM manganese (55) and will be present in variable amounts depending on the cell line and treatment protocol.

How does high cytosolic iron cause decreased mitochondrial manganese accumulation? Mammals mediate high affinity mitochondrial iron uptake via mitoferrin (56). Deletion or mutation of mitoferrin in zebrafish results in erythropoietic defects and reduced mitochondrial iron levels (56). The decreased uptake of manganese probably results from a competition for uptake after the mitoferrin system becomes saturated, at site(s) of additional low affinity iron transport. One such low affinity transporter of iron must be the unknown primary manganese transporter. Deletion of Mrs3/4, the yeast homologues of mitoferrin, in an iron overload model causes an increase in the activity of SOD2—suggesting conserved mechanisms may be involved in balancing iron and manganese availability in the mitochondria (48).

In summary, we have demonstrated that iron accumulation in a mouse model of hemochromatosis is confined to the cytoplasm, while mitochondrial iron content is maintained at normal levels. However, *Hfe*$^{-/-}$ mutant mice are significantly deficient in mitochondrial manganese, copper, and zinc, resulting in mitochondrial dysfunction and impairment of mitochondrial-dependent activities such as insulin secretion. Our present findings suggest a new component to iron toxicity, namely altering mitochondrial metal content—resulting in attenuated mitochondrial antioxidant defenses and overall function. The deficiencies of manganese, copper, and zinc in mitochondria from *Hfe*$^{-/-}$ mice are new factors in understanding the pathogenesis of hemochromatosis and possibly other diseases characterized by altered metal homeostasis, mitochondrial dysfunction, and oxidative stress. Interactions among these metal transport mechanisms could explain, for example, why individuals with hemochromatosis are more susceptible to amyotrophic lateral sclerosis (57), a disease whose familial form is caused by mutations in the Cu/ZnSOD gene (58). The further consequences of, and potential ability to correct, these abnormalities in mitochondrial metal content are under investigation and represent a potential for therapeutic intervention.

ACKNOWLEDGMENTS

This work was supported by grants from the National Institutes of Health (DK59512, DAM.; CA61286, DRW), the Research Service of the Veterans Administration, and the Ben B and Iris M Margolis Foundation.

REFERENCES

1. Andrews NC. (1999) Disorders of iron metabolism. *N. Engl. J. Med*. 341:1986–95.
2. Bothwell TH, Charlton RW, Motulsky AG. (1995) Hemochromatosis. In: Scriver CR, Beaudet AL, Sly WS, Valle D (ed.) *The metabolic and molecular bases of inherited disease*. 7th ed. Vol. 2. McGraw-Hill, New York, pp. 2237–69.
3. Feder JN et al. (1997) The hemochromatosis founder mutation in HLA-H disrupts beta2-microglobulin interaction and cell surface expression. *J. Biol. Chem*. 272:14025–8.
4. Nemeth E et al. (2004) Hepcidin regulates cellular iron efflux by binding to ferroportin and inducing its internalization. *Science*. 306:2090–3.
5. McClain DA et al. (2006) High prevalence of abnormal glucose homeostasis secondary to decreased insulin secretion in individuals with hereditary haemochromatosis. *Diabetologia*. 49:1661–9.
6. Feder JN et al. (1996) A novel MHC class I-like gene is mutated in patients with hereditary haemochromatosis. *Nat. Genet*. 13:399–408.
7. Cartwright GE et al. (1979) Hereditary hemochromatosis. Phenotypic expression of the disease. *N. Engl. J. Med*. 301:175–9.
8. Baynes JW. (1991) Role of oxidative stress in development of complications in diabetes. *Diabetes*. 40:405–12.
9. Graf E, Mahoney JR, Bryant RG, Eaton JW. (1984) Iron-catalyzed hydroxyl radical formation. Stringent requirement for free iron coordination site. *J. Biol. Chem*. 259:3620–4
10. Balla G, Vercellotti GM, Eaton JW, Jacob HS. (1990) Iron loading of endothelial cells augments oxidant damage. *J. Lab. Clin. Med*. 116:546–54.
11. Cooksey RC et al. (2004) Oxidative stress, beta-cell apoptosis, and decreased insulin secretory capacity in mouse models of hemochromatosis. *Endocrinology*. 145:5305–12.
12. Levy JE, Montross LK, Cohen DE, Fleming MD, Andrews NC. (1999) The C282Y mutation causing hereditary hemochromatosis does not produce a null allele. *Blood*. 94:9–11.
13. Pelot D, Zhou XJ, Carpenter P, Vaziri ND. (1998) Effects of experimental hemosiderosis on pancreatic tissue iron content and structure. *Dig. Dis. Sci*. 43:2411–4.
14. Cobine PA, Ojeda LD, Rigby KM, Winge DR. (2004) Yeast contain a non-proteinaceous pool of copper in the mitochondrial matrix. *J. Biol. Chem*. 279:14447–55.
15. Boudina S, Sena S, O'Neill BT, Tathireddy P, Young ME, Abel ED. (2005) Reduced mitochondrial oxidative capacity and increased mitochondrial uncoupling impair myocardial energetics in obesity. *Circulation*. 112:2686–95.
16. Veeger CV, Zeylemaker WP. (1969) Determination of Succinate with Succinate Dehydrogenase. *Methods Enzymol*. 13:524–5.
17. Darley-Usmar VM, Rickwood D, Wilson MT. (1987) *Mitochondria*: *A Practical Approach*. IRL Press Oxford.
18. Chabrashvili T et al. (2003) Effects of ANG II type 1 and 2 receptors on oxidative stress, renal NADPH oxidase, and SOD expression. *Am. J. Physiol. Regulatory Integrative Comp. Physiol*. 285:117–24.
19. Esparza JL, Gomez M, Rosa Nogues M, Paternain JL, Mallol J, Domingo JL. (2005) Melatonin reduces oxidative stress and increases gene expression in the cerebral cortex and cerebellum of aluminum-exposed rats. *J. Pineal. Res*. 39:129–36.
20. Lund AK, Peterson SL, Timmins GS, Walker MK. (2005) Endothelin-1-mediated increase in reactive oxygen species and NADPH Oxidase activity in hearts of aryl hydrocarbon receptor (AhR) null mice. *Toxicol. Sci*. 88:265–73.
21. Lekanne Deprez RH, Fijnvandraat AC, Ruijter JM, Moorman AF. (2002) Sensitivity and accuracy of quantitative real-time polymerase chain reaction using SYBR green I depends on cDNA synthesis conditions. *Anal. Biochem*. 307:63–9.
22. Cooksey RC, Pusuluri S, Hazel M, McClain DA. (2006) Hexosamines Regulate Sensitivity of Glucose-Stimulated Insulin Secretion in Beta Cells. *Am. J. Physiol. Endocrinol. Metab*. 290:E334–40.
23. Tang J, Pugh W, Polonsky KS, Zhang H. (1996) Preservation of insulin secretory responses to P2 purinoceptor agonists in Zucker diabetic fatty rats. *Am. J. Physiol*. 270:E504–12.
24. Barros MH, Bandy B, Tahara EB, Kowaltowski AJ. (2004) Higher respiratory activity decreases mitochondrial reactive oxygen release and increases life span in Saccharomyces cerevisiae. *J. Biol. Chem*. 279:49883–8.
25. Nojiri H et al. (2006) Oxidative stress causes heart failure with impaired mitochondrial respiration. *J. Biol. Chem*. 281:33789–801.
26. Gardner PR, Nguyen DH, White CW. (1994) Aconitase is a Sensitive and Critical Target of Oxygen Poisoning in Cultured Mammalian Cells and in Rat Lungs *PNAS* 91:12248–52.

27. Maechler P, Wollheim CB. (2001) Mitochondrial function in normal and diabetic beta-cells. *Nature*. 414:807–12.
28. Wollheim CB. (2000) Beta-cell mitochondria in the regulation of insulin secretion: a new culprit in type II diabetes. *Diabetologia*. 43:265–77.
29. Desagher S, Martinou JC. (2000) Mitochondria as the central control point of apoptosis. *Trends Cell Biol*. 10:369–77.
30. Orth M, Schapira AH. (2001) Mitochondria and degenerative disorders. *Am. J. Med. Genet*. 106:27–36.
31. Marin-Garcia J, Goldenthal M. (2004) Mitochondria play a critical role in cardioprotection. *J. Card. Fail*. 10:55–66.
32. Kennedy ED, Maechler P, Wollheim CB. (1998) Effects of depletion of mitochondrial DNA in metabolism secretion coupling in INS-1 cells. *Diabetes*. 47:374–80.
33. Soejima A et al. (1996) Mitochondrial DNA is required for regulation of glucose-stimulated insulin secretion in a mouse pancreatic beta cell line, MIN6. *J. Biol. Chem*. 271:26194–9.
34. Lowell BB, Shulman GI. (2005) Mitochondrial dysfunction and type 2 diabetes. *Science*. 307:384–7.
35. Luft R. (1994) The Development of Mitochondrial Medicine. *PNAS* 91: 8731–8.
36. James AM, Murphy MP. (2002) How mitochondrial damage affects cell function. *J. Biomed. Sci*. 9:475–87.
37. Houstis N, Rosen ED, Lander ES. (2006) Reactive oxygen species have a causal role in multiple forms of insulin resistance. *Nature*. 440:944–8.
38. Schafer FQ, Buettner GR. (2000) Acidic pH amplifies iron-mediated lipid peroxidation in cells. *Free Radic. Biol. Med*. 28:1175–81.
39. Lucas DT, Szweda LI. (1998) Cardiac reperfusion injury: aging, lipid peroxidation, and mitochondrial dysfunction. *Proc. Natl. Acad. Sci. U. S. A*. 95:510–4.
40. Fridovich I. (1995) Superoxide radical and superoxide dismutases. *Annu. Rev. Biochem*. 64:97–112.
41. Li Y et al. (1995) Dilated cardiomyopathy and neonatal lethality in mutant mice lacking manganese superoxide dismutase. *Nat. Genet*. 11:376–81.
42. Van Remmen H, Salvador C, Yang H, Huang TT, Epstein CJ, Richardson A. (1999) Characterization of the antioxidant status of the heterozygous manganese superoxide dismutase knockout mouse. *Arch. Biochem. Biophys*. 363:91–7.
43. Kokoszka JE, Coskun P, Esposito LA, Wallace DC. (2001) Increased mitochondrial oxidative stress in the Sod2 (+/–) mouse results in the age-related decline of mitochondrial function culminating in increased apoptosis. *Proc. Natl. Acad. Sci. U. S. A*. 98:2278–83.
44. Williams MD, Van Remmen H, Conrad CC, Huang TT, Epstein CJ, Richardson A. (1998) Increased oxidative damage is correlated to altered mitochondrial function in heterozygous manganese superoxide dismutase knockout mice. *J. Biol. Chem*. 273:28510–5.
45. Huang J et al. (2007) Increased glucose disposal and AMP-dependent kinase signaling in a mouse model of hemochromatosis. *J. Biol. Chem*. 282:37501–7
46. Whittaker JW. (2003) The irony of manganese superoxide dismutase. *Biochem. Soc. Trans*. 31:1318–21.
47. Luk E, Yang M, Jensen LT, Bourbonnais Y, Culotta VC. (2005) Manganese activation of superoxide dismutase 2 in the mitochondria of Saccharomyces cerevisiae. *J. Biol. Chem*. 280:22715–20.
48. Yang M et al. (2006) The effects of mitochondrial iron homeostasis on cofactor specificity of superoxide dismutase 2. *EMBO J*. 25:1775–83.
49. Vance CK, Miller AF. (1998) Spectroscopic comparisons of the pH dependencies of Fe-substituted (Mn) superoxide dismutase and Fe-superoxide dismutase. *Biochemistry*. 37:5518–27.
50. Irazusta V, Cabiscol E, Reverter-Branchat G, Ros J, Tamarit J. (2006) Manganese is the link between frataxin and iron-sulfur deficiency in the yeast model of Friedreich's ataxia. *J. Biol. Chem*. 281:12227–32.
51. Beyer WF, Fridovich I. (1991) In vivo competition between iron and manganese for occupancy of the active site region of the manganese-superoxide dismutase of Escherichia coli. *J. Biol. Chem*. 266:303–8.
52. Mizuno K, Whittaker MM, Bachinger HP, Whittaker JW. (2004) Calorimetric studies on the tight binding metal interactions of Escherichia coli manganese superoxide dismutase. *J. Biol. Chem*. 279:27339–44.
53. Privalle CT, Fridovich I. (1992) Transcriptional and maturational effects of manganese and iron on the biosynthesis of manganese-superoxide dismutase in Escherichia coli. *J. Biol. Chem*. 267:9140–5.
54. Dobson AW, Erikson KM, Aschner M. (2004) Manganese neurotoxicity. *Ann. N. Y. Acad. Sci*. 1012:115-128.
55. Prohaska JR. (1987) Functions of trace elements in brain metabolism. *Physiol. Rev*. 67:858–901.
56. Shaw GC et al. (2006) Mitoferrin is essential for erythroid iron assimilation. *Nature*. 440:96–100.
57. Wang XS et al. (2004) Increased incidence of the Hfe mutation in amyotrophic lateral sclerosis and related cellular consequences. *J. Neurol. Sci*. 227:27–33.
58. Rosen DR et al. (1993) Mutations in Cu/Zn superoxide dismutase gene are associated with familial amyotrophic lateral sclerosis. *Nature*. 362:59–62.